Modelling of Ice-Melting Circuit under Influence of EMF Induced by the Currents of Overhead Lines

NIKOLAY V. KOROVKIN, VALERIY O. GONCHAROV[1], NIKOLAY V. SILIN[2]
1) Theoretical Electrical Engineering Department
St. Petersburg State Polytechnic University
29, Polytechnicheskaya st., 195251, St.Petersburg
2) Theoretical Electrical Engineering Department
Far Eastern Federal University
8, Suhanova st., 690950, Vladivostok
RUSSIAN FEDERATION
Nikolay.Korovkin@gmail.com, Valeriy.Goncharov@me.com, Silin22@mail.ru

Abstract: - To prevent icing of TL (transmission lines) and GW (ground wires) during certain weather conditions the de-icing procedure is needed. The currents of operating TL influence on the de-icing process. A mathematical model was developed which makes possible the estimation of this influence. The main ice-melting diagrams are considered. The methodology of determination of induced EMF value in ice-melting loop is described. Ice-melting current curves under different conditions are compared and analyzed.

Key-Words: - ice melting, ground wire, ice-melting circuit, induced EMF

1 Introduction

The ice covering represents a huge danger to the power systems' operation. It can lead to the wires breakage and even to the towers destruction. In December 2001, the ice covering brought to the damage of TL (transmission lines) of total length 2500 km in Sochi. In early 2008, a severe ice storm occurred in Southern China, which caused at least 7541 TL above 10 kV and 859 substations above 35 kV to be out of service [1].

The necessity of GW (ground wires) de-icing is more urgent because there are no currents flowing during normal operation mode through GW as opposed to TL. Also, while TL wires are usually made of aluminum-conductor steel-reinforced cable, the GW are often made of steel, so their conductance is lower. This fact was already studied in [2] and has been considered in calculations with higher electrical resistivity of GW.

The de-icing method using DC is most commonly used. DC is used more often than AC for the ice-melting procedures because the heating current adjustment is very limited in case of using AC [3]. The basic ice-melting diagram is given on Fig.1. The typical diagrams are given in Table 1.

The ice-melting current value is estimated with the following approximate expression [3]:

$$I \cong \pi \left[0.5\sigma d \left(T_{\max}{}^{4} - T_{\mathrm{amb}}{}^{4} \right) + \frac{\lambda_{\mathrm{a}} \mathrm{Nu} \left(T_{\max} - T_{\mathrm{amb}} \right)}{R_T} \right]^{0.5} \quad (1)$$

where R_T, Ω, is the resistivity of GW under maximum allowed temperature $T_{\max}$, K; $\sigma = 5.67 \cdot 10^{-8}$ $\mathrm{W \cdot m^{-2} \cdot} K^{-4}$ is Stefan-Boltzmann constant; d is a GW diameter, m; T_{amb} is an ambient temperature, K; λ_{a} is an air thermal conductivity, $\mathrm{W{\cdot}m^{-1}K^{-1}}$; Nu is Nusselt number:

$$\mathrm{Nu} = 0.65\,\mathrm{Re}^{0.2} + 0.23\,\mathrm{Re}^{0.61} \quad (2)$$

where Re is Reynolds number:

$$\mathrm{Re} = 1.644 \cdot 10^{9}\, v\, d \left[T_{\mathrm{amb}} + 0.5 \left(T_{\max} - T_{\mathrm{amb}} \right) \right]^{-1.78} \quad (3)$$

where v is a wind velocity, $\mathrm{m{\cdot}s^{-1}}$.

2 Purpose of Work

It is desirable to conduct the GW ice-melting procedure without powering down the TL. The currents in the wires of the TL, located on the same tower as the GW, and the currents of the neighboring TL induce the EMF in the ice-melting loop (Fig.1). This can lead to the rectifier's breakdown while engaging as well as while operating. The aim of this paper is an estimation of the EMF value induced in the ice-melting loop under different conditions (such as different TL operation modes, different TL types and different ice-melting diagrams) and the development of an application to estimate the induced EMF value.

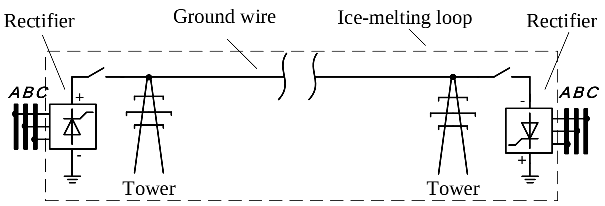

Fig.1. Basic ice-melting diagram.

Table 1. Ice-Melting Circuit Diagrams

Name of the diagram	Diagrams
GW-ground	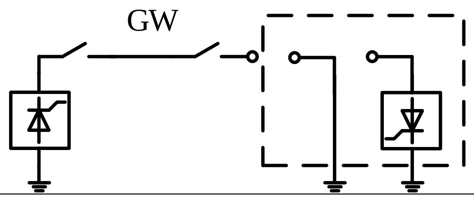
GW1,2-ground	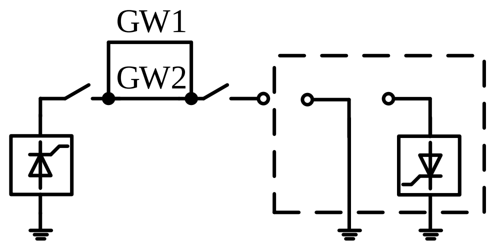
GW1,2	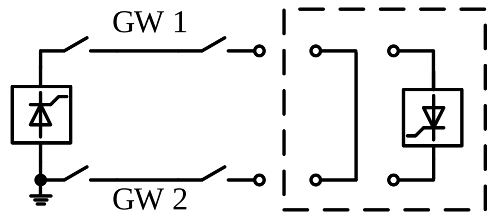

3 Modelling of Ice-Melting Circuit

The rectifier may be powered through distribution bus of electrical substation as well as by a diesel generator. Transformers are used only in case of absence of distribution bus of needed voltage. Fig.2 shows an example of rectifier connection. Electrical substation has a step-down transformer T2, its high-voltage winding is connected to distribution bus II, low-voltage winding feeds distribution bus 10 kV. Bridge rectifier BR is powered by that bus. Reactor's inductive resistance X_R is connected in series. Rectified current I_d flows through GW with active resistance R_d and reactance X_d.

In present paper we consider that three-phase full-wave bridge rectifier is powered by power network. In equivalent circuit shown on Fig. 3 the whole power network is replaced by 3-phase symmetrical system of voltage sources with proper impedance X_γ. Reactor's impedance is represented by X_R. However, due to energy saving approach it is not used in most cases, so in further we will neglect it. Switches *K1* and *K2* commutate rectifier and GW.

Models of controlled valves *V1-V6* are based on idea of "ideal valves". We assume that "ideal valve" has the following properties:

1) In forward conducting mode, when the valve has been triggered into conduction, its impedance is zero and will remain such until the forward current drops below zero.
2) In reverse blocking mode, when voltage is applied in the direction that would be blocked by a diode, its impedance is so high that the reverse current may be neglected.
3) In forward blocking mode, when voltage is applied in the direction that would cause a diode to conduct, but the valve has not been triggered into conduction, its impedance is not affected and remains high.
4) After valve has been fired it cannot be blocked by the trigger.

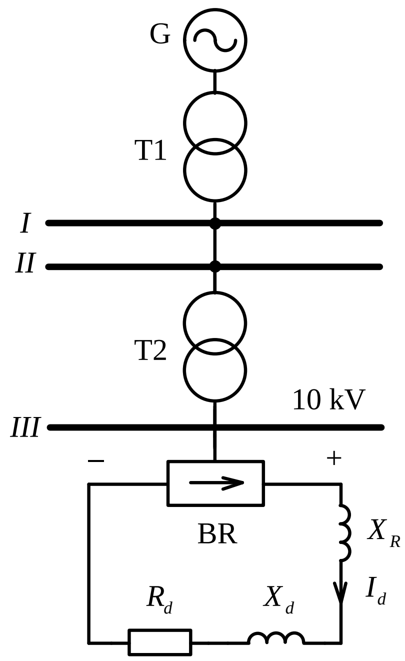

Fig.2. Connection diagram of rectifier to power network.

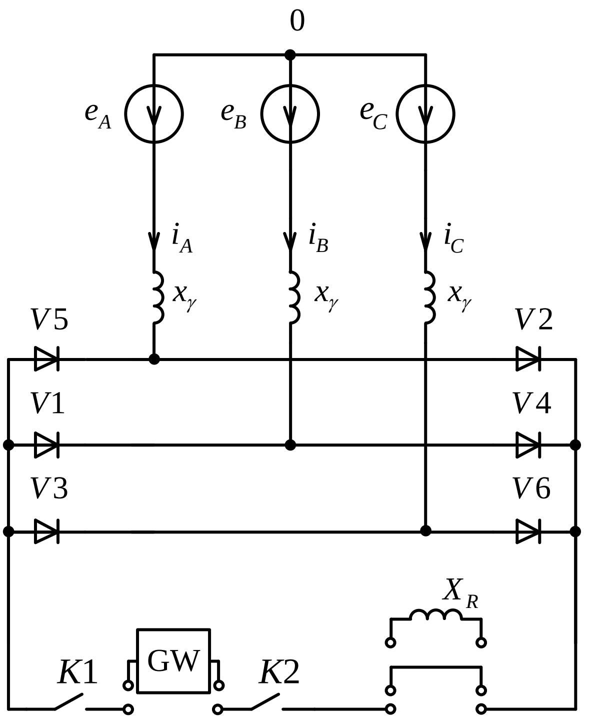

Fig.3. Equivalent circuit of ice-melting circuit.

4 Modelling of Controlled Valve

The equivalent valve model is shown on Fig.4. In that model $R \gg r$ .Value of r is selected to be much less than any other resistance in circuit. When valve is open, the switch *K1* is closed and total resistance of the model $R_{model} \approx r$. While value of the current I is positive, the valve still conducts. When the current's direction changes, the valve is closed, switch *K1* becomes opened and $R_{model} \approx R$. While voltage U is negative, the valve stays opened. In moment when voltage value U changes sign (natural firing instant), the valve becomes open, or, in case if controlling angle $\alpha \neq 0$, countdown of delay time t_{delay} starts, which is followed by triggering pulse. If by that time voltage U is positive, the valve becomes opened.

Delay time is calculated with an expression:

$$t_{delay} = \frac{\alpha}{360\ f}, \tag{4}$$

where α is the controlling angle, deg; f is the frequency, Hz.

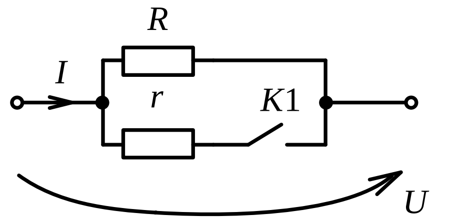

Fig.4. Equivalent model of the valve.

5 Modelling of Ground Wires

Model of GW has resistance, self and mutual inductance parameters. While modelling, we should take into account properties of wires as well as of a ground. We consider ground to be a perfect conductor ($\gamma = \infty$). In this case, we can implement method of images [4]. Equivalent figures of disposition of the wires and their images are shown on Fig.5. Considering the fact that the TL wires are loaded, the current which may be excited in them by ice-melting current flowing in GW is rather small according to our estimations. It means that influence of this current on magnetic flux of loop $GW^{(1)}$–$GW^{(2)}$ on Fig.5(a) is negligible. Thus the influence on inductance of that loop is negligible too.

Resistance may be calculated using simple expression:

$$R = \rho \frac{l}{S} \tag{5}$$

where ρ is the electrical resistivity, Ω·m; l is the length of the wire, m; S is the cross-section area of the wire, m^2.

Self inductance may be calculated using expression:

$$L = \frac{\mu_0 l}{2\pi}\left(\ln\frac{2l}{r} - 1\right) + \frac{\mu l}{8\pi} \tag{6}$$

where $\mu_0 = 4\pi \cdot 10^{-7}\ \mathrm{H \cdot m^{-1}}$ is the magnetic constant; r is the radius of the wire, m; μ is the magnetic permeability of the wire's material, $H \cdot m^{-1}$.

Resistance and self inductance of the wires depend on properties of the wires (such as material, radius and length), but the mutual inductance is determined by the mutual disposition of the wires (that is, distances D_{kq} between wires k and q as shown on Fig.6). To calculate it, we may use the following expression:

$$M_{k-q} = \frac{\Phi_{k-q}}{i} \tag{7}$$

where M_{k-q} is the mutual inductance between wires k and q, Φ_{k-q} is the magnetic flux created by current i through area between wires k and q.

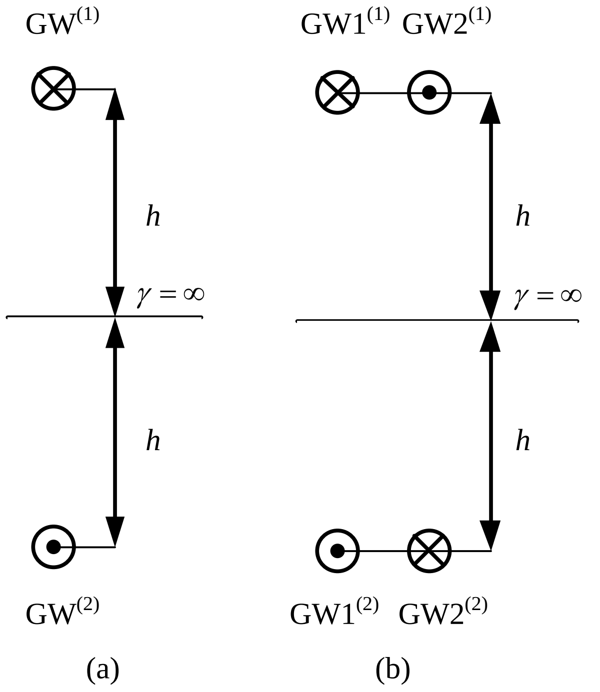

Fig.5. Equivalent figures of disposition of wires and their images. (a) For GW–ground diagram. (b) For GW1,2–ground and GW1,2 diagrams.

As seen on Fig.6:

$$D_{12} = D_{21} = D_{34} = D_{43} = D_1,$$
$$D_{13} = D_{31} = D_{23} = D_{32} = D_2,$$
$$D_{14} = D_{41} = D_{24} = D_{42} = D_3.$$

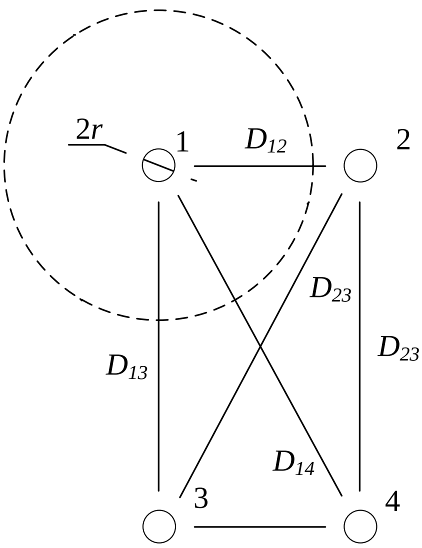

Fig.6. Mutual disposition of the wires for diagrams GW1,2 and GW1,2–ground.

We may conclude that

$$M_{1-2} = M_{3-4} = M_{3-4} = M_{1-2} = M_1,$$
$$M_{1-3} = M_{2-4} = M_{2-4} = M_{1-3} = M_2,$$
$$M_{1-4} = M_{2-3} = M_{2-3} = M_{1-4} = M_3.$$

Equivalent circuits of GW are given on Fig.7.

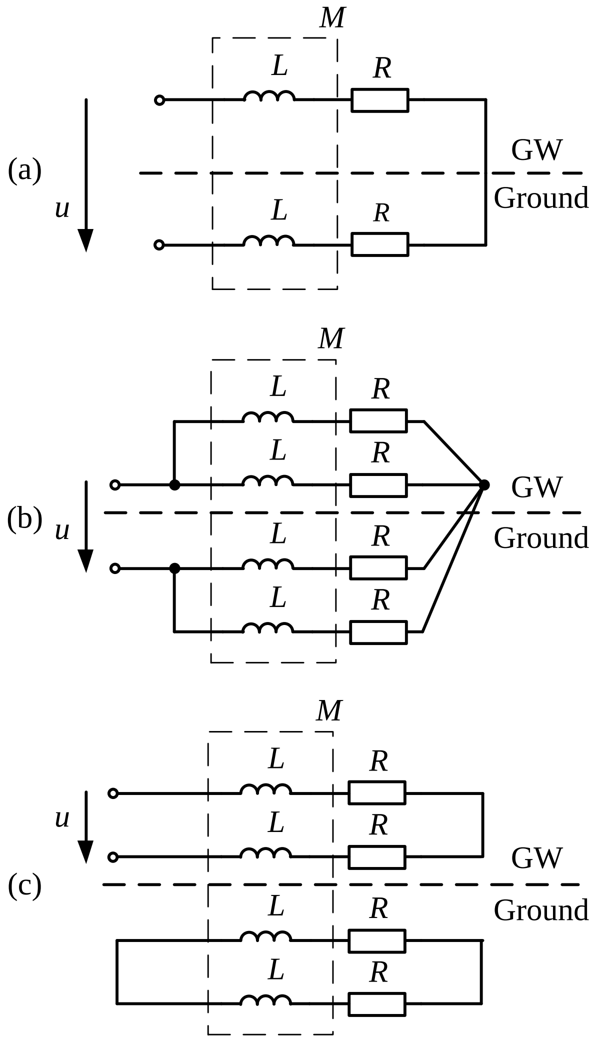

Fig.7. Equivalent circuits of GW. (a) For GW–ground diagram. (b) For GW1,2 diagram. (c) For GW1,2–ground diagram.

6 Induced EMF Calculation Method

The induced EMF value in the ice-melting loop is determined by a magnetic flux Φ (which is created by the TL currents) through the surface whose boundary is the ice-melting loop [4]. The most significant factors, which determine the values of magnetic flux and EMF, are currents' values, their phase lags, and distance between the ice-melting loop and the TL wires. The calculation method rests on the following assumptions:

1) the TL currents form the balanced three-phase system;
2) because the currents' phase lags of all TL are not defined, we consider that the currents of the same phase index of the different circuits and of different towers have the same phase lag;
3) all TL wires and GW are rectilinear (we neglect the wires' deflection).

Also, an influence of the ground should be taken into account. In this paper we consider that the ground is a perfect conductor ($\gamma = \infty$). Hence, we may implement the method of images [4]. The resulting picture in case of using ice-melting diagram GW–ground is shown on Fig.8 [11]. With assumptions stated previously, the induced EMF value can be calculated analytically [4]:

$$\dot{\Phi}_B = \left(\dot{A}_1 - \dot{A}_2\right) l = \left(\frac{\mu_0}{2\pi} \sum_{k=1}^{6} \dot{I}_k \ln r_k^{(1)} - \frac{\mu_0}{2\pi} \sum_{k=1}^{6} \dot{I}_k \ln r_k^{(2)} \right) l \quad (8)$$

where l is the length of the parallel TL and GW, m; A_1, A_2 are the vector potential values on the GW and its image respectively, Wb·m^{-1}; $r_k^{(1)}$, $r_k^{(2)}$ ($k = 1 \div 6$) are the distances shown on Fig.8, m.

The induced EMF value:

$$E = \left|\dot{E}\right| = \left|-j\omega \cdot \dot{\Phi}_B\right| = \omega \cdot \Phi_B \quad (9)$$

$$\omega = 2\pi \cdot f = 314 \text{ rad/s} \quad (10)$$

The RMS EMF value calculated in (9) is a result of the effect from one circuit of one TL. After that, we can calculate the influence from the other circuit of multiple TL and, taking into consideration the assumption 2, sum both reactions. Obviously, the result will be the majoring one. After calculating induced EMF values, we can put voltage sources of corresponding amplitude into equivalent circuit of GW shown on Fig.7 and then solve it.

7 Induced EMF Values Calculation Results

The calculations of induced EMF values were made using the application developed specifically for the present paper that includes:
1) the TL map;
2) the TL data such as types of GW, wires and towers as well as a transposition data;
3) the nominal currents, voltages and electric power transported through TL.

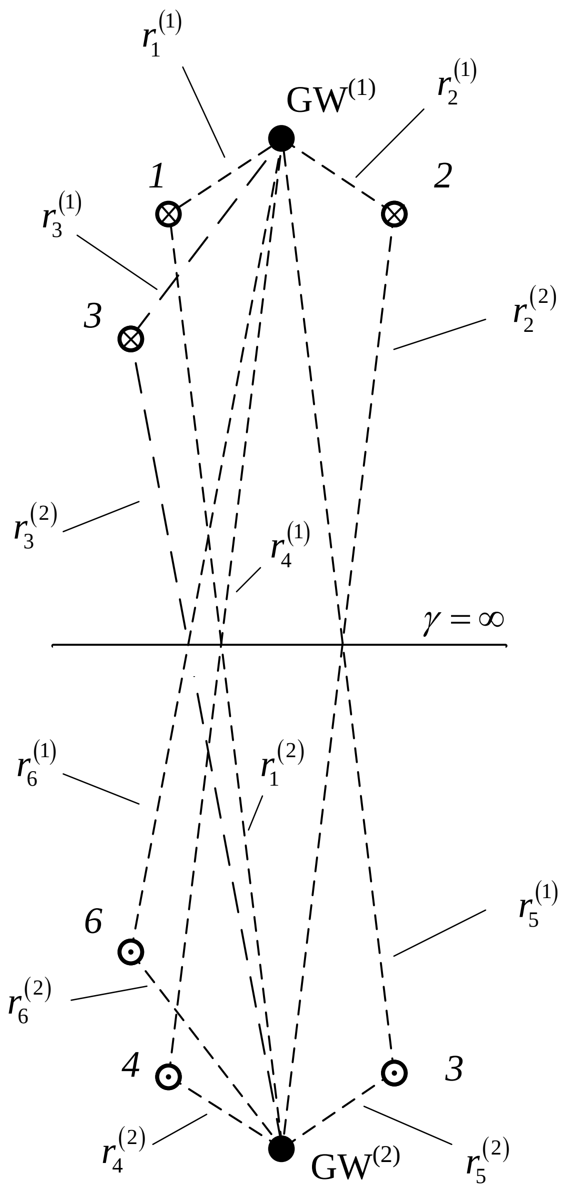

Fig.8. Positional relationship of TL wires, GW and their images in case of using "GW–ground" ice-melting diagram. $GW^{(1)}$ – the ground wire, 1,2,3 – the TL wires, $GW^{(2)}$ – image of the ground wire, 4,5,6 – the images of TL wires.

Fig.9(a) represents a map of a power system span in Moscow Oblast. TL 1, which is located on the same tower as GW in question, is located near TL 2, 3 and 4. All of them operate in nominal modes. Fig.9(a) also contains the information of the nominal currents' values. Fig.9(b) represents the tower dimensions.

The minimum distance allowed between the wires of neighboring 220 kV towers is 7 meters [5]. We consider that all towers are located in such a way that this condition is met for all TL.

The calculations for ice-melting diagrams from Table 1 and two variants of phase disposition (see Fig.10) are represented in Table 2 [12].

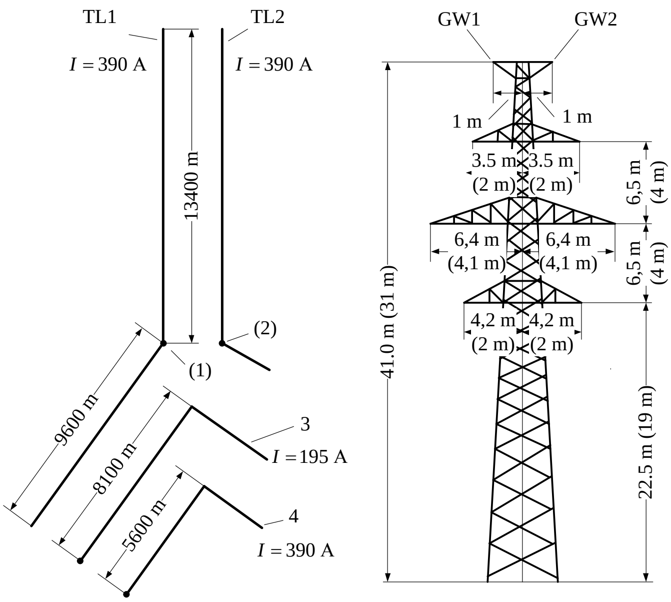

(a) (b)

Fig.9. Calculation data. (a) The map of a power system span. TL 1, TL 2, TL 4 – double-circuit TL 220 kV, TL 3 – double-circuit TL 110 kV. (b) The dimension of the towers used. The dimensions for 110 kV towers are given within brackets.

Table 2. Calculation Results for Normal Mode

№	Ice melting diagram	Phase disposition	Induced EMF value (RMS), kV
1	GW–ground	a	2.4
2	GW–ground	b	0.9
3	GW1,2–ground	a	2.4
4	GW1,2–ground	b	0.8
5	GW1,2	a	0.1
6	GW1,2	b	0.01

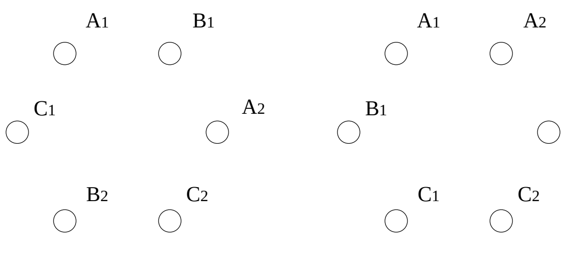

(a) (b)

Fig.10. Variants of phases' disposition. (a) The first variant. (b) The second variant.

EMF values vary from insignificant 0.01 kV to 2.4 kV. The lowest values correspond to diagram GW1,2 due to the minimal ice melting loop area comparing to other ones.

In case of short circuit in TL1 (point (1) on Fig.9) and TL2 (point (2) on Fig.9) of value 20 kA the induced EMF values are much higher (see Table 3 [12]). For the cases of using ice-melting diagram GW1,2 the induced EMF values are comparable to the highest values for the normal operational modes (see Table 2). In other cases, the values are significant. Due to the power-system protection quick response, they cannot alter much the de-icing process. However, such high voltages represent a danger to the rectifier and may be the reason of rectifier's breakdown. Such events were recorded to occur.

Table 3. Calculation Results for Abnormal Mode

№	Ice melting diagram	Point of short circuit	Induced EMF value (RMS), kV
1	GW–ground	1	82
2	GW–ground	2	51
3	GW1,2–ground	1	83
4	GW1,2–ground	2	51
5	GW1,2	1	3
6	GW1,2	2	2

8 Equivalent Circuit Parameters

The equivalent circuit shown on Fig.3 has the following parameters: $E_m = 14.85$ kV , $x_\gamma = 0.0716\ \Omega$.

For calculation of the parameters of the GW we considered a wire with a radius $r = 6{,}25 \cdot 10^{-3}$ m, cross-section area $S = 1{,}0797 \cdot 10^{-4}\ \text{m}^2$, resistivity $\rho = 2 \cdot 10^{-7}\ \Omega \cdot \text{m}$ and magnetic permeability $\mu_r = 220$. For GW located on the same towers as TL1 with total length $l = 23 \cdot 10^3$ m we got the following parameters:

$$R = \rho \frac{l}{S} = 2 \cdot 10^{-7} \cdot \frac{23 \cdot 10^3}{1{,}0707 \cdot 10^{-4}} = 4{,}260 \cdot 10^1\ \Omega.$$

$$L = \frac{\mu_0 l}{2\pi}\left(\ln \frac{2l}{r} - 1 + \frac{\mu_r}{4}\right) =$$

$$= \frac{4\pi \cdot 10^{-7} \cdot 23 \cdot 10^3}{2\pi}\left(\ln \frac{2 \cdot 23 \cdot 10^3}{6{,}25 \cdot 10^{-3}} - 1 + \frac{220}{4}\right) =$$

$$= 3{,}211 \cdot 10^{-1}\ \text{H}.$$

The mutual inductances for tower with dimensions as shown on Fig.9(b) are:

$$M_1 = 2,493 \cdot 10^{-2} \text{ H},$$

$$M_2 = 4,362 \cdot 10^{-2} \text{ H},$$

$$M_3 = 4,362 \cdot 10^{-2} \text{ H}.$$

9 Results

Unaffected and affected by induced EMF of values from Table 2 curves of ice-melting current for different diagrams and phase disposition variants are shown on Fig.11–16. RMS values of ice-melting current are given in Table 4.

Table 4. RMS Values of Ice-Melting Current under Different Conditions

№	**Ice melting diagram**	***E=0***	***E≠0***	
			1st phases' disposition variant	**2nd phases' disposition variant**
1	GW–ground	24.62 A	26,80 A	24.80 A
2	GW1,2–ground	24.83 A	41.20 A	27.07 A
3	GW1,2	24.64 A	24.64 A	24.63 A

In worst case, the induced EMF increases RMS value of melting current up to 66% (diagram type GW1,2–ground). The least changing happens in case of GW1,2 diagram (almost no difference). In case of GW–ground diagram, the changing is up to 9%.

Increasing of ice-melting current speeds up the de-icing process. When there is no monitoring equipment, the ice melting procedure is conducted for an estimated time. Therefore, if the ice will be melted earlier than predicted, the wire will experience the unwanted heating. Excess heating decreases durability and lifetime of the wires.

10 Discussion

We calculated the induced EMF values supposing that the ground is a perfect conductor. In real situations, the ground has limited conductivity. The influence of the ground was studied in [6]–[8]. For frequencies concerned in present paper consideration of this influence can't considerably affect the results. Nevertheless, this consideration is needed. Its realization according to methods described in [9]–[11] does not represent fundamental problems and is planned for accomplishing in authors' future papers.

Also, taking into account parameters of grounding systems of power lines will allow us to increase accuracy of the model [10].[13]. Future model development may require implementing EMF calculation methods in grounding systems too [14]. Different circuit modeling techniques are given in [15]–[18] and can also be used for model improvements.

The other concern represents taking into account the capacity of the wires. According to our estimations, because the ice-melting procedure is usually conducted in relatively short sections (dozens of km), GW are located quite high and they are thinner than TL wires, consideration of the capacity will not change calculated ice-melting current. However, a possibility of occurrence of resonance of harmonics of 6ω should be studied. Estimation of the possibility of these occurrences requires complex calculations, as well as consideration of ground influence. The completion of such calculations is planned to be done in future.

In present paper we did not examined the ice-melting current as a source of disturbance for TL operation. This noise may possibly overload filters of high-frequency communication system through TL wires or influence the operation of instrument transformers. Problems of radiation of power equipment in wide frequency range were discussed in [19]-[21]. Problem for additional EM radiation of TL wires under influence of de-icing process is also planned to be examined in future.

11 Conclusions

When ice-melting procedure using rectifiers is going to be conducted, the induced EMF in GW from currents of neighboring TL should be taken into account.

The danger of inducing high EMF values in GW1,2 ice-melting diagram is significantly less than in GW–ground and GW1,2–ground loops.

When the ice-melting procedure is conducted, a short circuit current in any TL, which is parallel to the GW, induces EMF high enough to damage a rectifier.

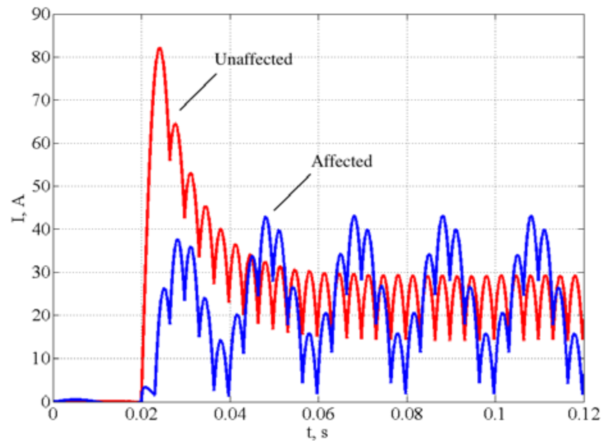

Fig.11. Affected by induced EMF and unaffected curves of ice-melting current for GW–ground diagram and 1st phases' disposition variant.

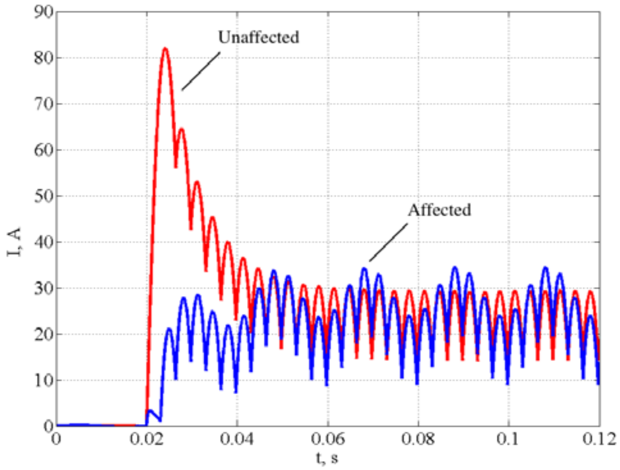

Fig.12. Affected by induced EMF and unaffected curves of ice-melting current for GW–ground diagram and 2nd phases' disposition variant.

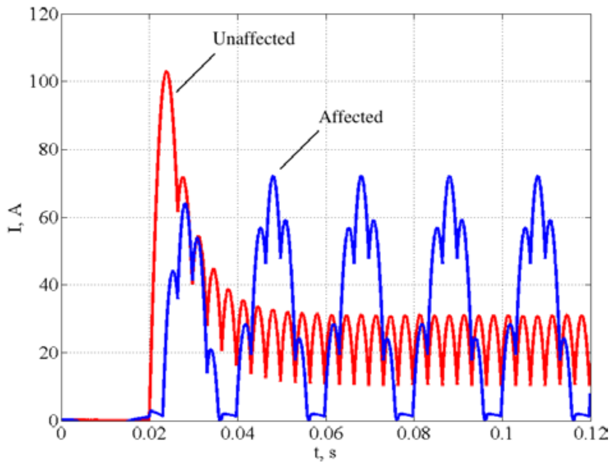

Fig.13. Affected by induced EMF and unaffected curves of ice-melting current for GW1,2–ground diagram and 1st phases' disposition variant.

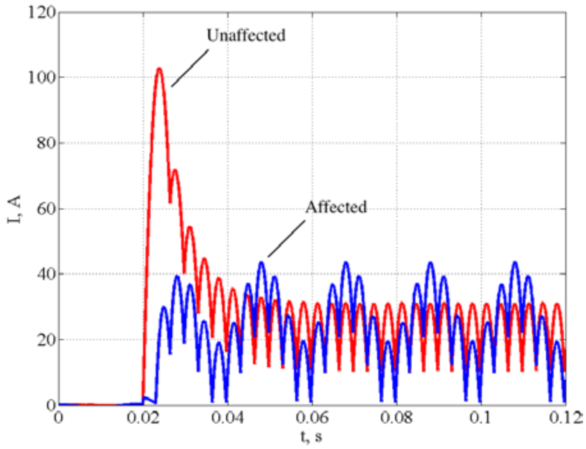

Fig.14. Affected by induced EMF and unaffected curves of ice-melting current for GW1,2–ground diagram and 2nd phases' disposition variant.

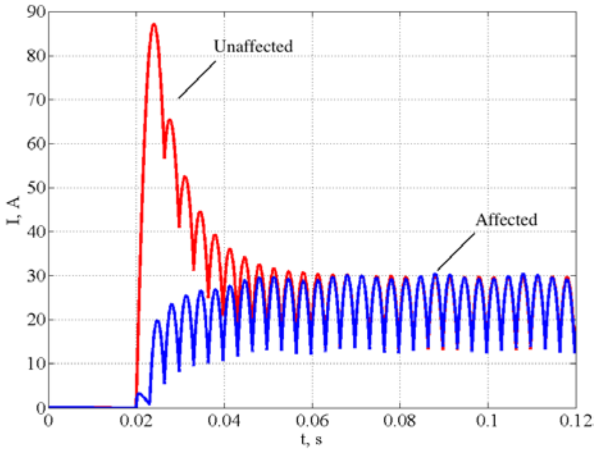

Fig.15. Affected by induced EMF and unaffected curves of ice-melting current for GW1,2 diagram and 1st phases' disposition variant.

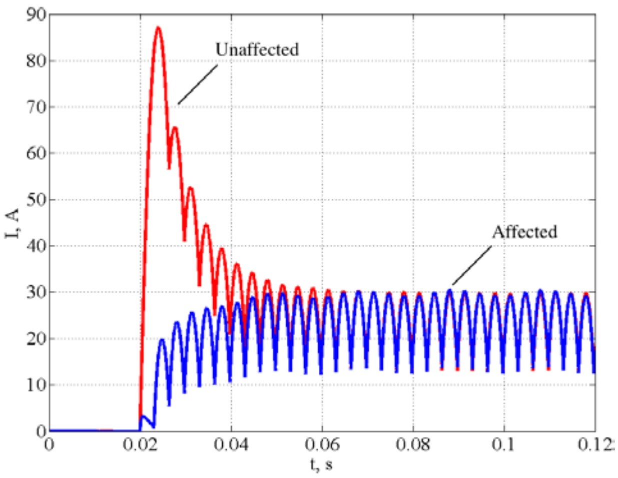

Fig.16. Affected by induced EMF and unaffected curves of ice-melting current for GW1,2 diagram and 2nd phases' disposition variant.

References:

[1] X. Shukai, Z. Jie, Review of Ice Storm Cases Impacted Seriously on Power Systems and De-Icing Technology, *Southern Power Syst. Technol.*, vol. 2, 2008, pp. 1–6.

[2] Dubitsky S.D., Korovkin N.V., Hayakawa M., Silin N.V. Thermal Resistance of Optical Ground Wire to Direct Lightning Strike, *International Symposium on Electromagnetic Theory, EMTS – Proceedings*, 2013, pp. 108–111.

[3] Federal Grid Company Standart 56947007–29.060.50.122–2012. *Ice-Melting Modes Calculation Methodology for Optical Ground Wires*, 2012.

[4] K.S. Demirchyan, L.R. Neumann, N.V. Korovkin., *Theoretical Foundations of Electrical Engineering*, Vol.1, Vol.2, Spb, 2009.

[5] *Rules of Electrical Installations Design*, Novosibirsk. 2009.

[6] Carson J.R. Wave Propagation in Overhead Wires with Ground Return, *Bell Syst. Technol. Journ*. Vol.5, no. 4, 1926, pp. 539–554.

[7] G.A. Grinberg, B.I. Bonshtedt, The Basis of the Exact Theory of the Wave Field of a Transmission Line, *JTPh*, Vol.24, no. 1, 1954, pp.67–95.

[8] H. Kikuchi, Wave Propagation along an Infinite Wire above Ground at High Frequencies, *Proc. Electrotech. J.*, Vol.2, 1956, 73–78.

[9] Korovkin N.V., Selina E.E. Efficient Method of Wave Processes in Transmission Line Simulation Using Discrete Models, *IEEE International Symposium on Electromagnetic Compatibility*, 1998, pp. 946–951.

[10] Korovkin N.V., Frolov O.V., Ivanova E.A., Shishiguin S.L. Computing Methods for Building Earthing Devices in Problems Related to EMC of Substations, *EMC EUROPE 2012 – International Symposium on Electromagnetic Compatibility*, Proceedings, 2012, pp. 863–866.

[11] Adalev A.S., Hayakawa M., Korovkin N.V., Identification of Electric Circuits: Problems and Methods of Solution Accuracy Enhancement, *Proceedings – IEEE International Symposium on Circuits and Systems, ISCAS*, 2005, pp. 980–983.

[12] Nikolay Korovkin, Valeriy Goncharov, Nikolay Silin, Estimation of Induced EMF Value in Ground Wire During Ice–Melting Procedure, *Book of Abstracts – International Conference on Mathematical Models and Methods in Applied Sciences, MMMAS*, 2014, p. 117.

[13] Netreba K.I., Korovkin N.V., Silin N.V., Modeling of Grounding Systems of Power Lines under Pulse Influence, *Book of Abstracts – International Conference on Mathematical Models and Methods in Applied Sciences, MMMAS*, 2014, p. 119.

[14] Korovkin N.V., Minevich T.G., Different Approaches for Calculation of EMF Induced by the Currents of Overhead Lines in the Shields of Buried Cables, *Book of Abstracts – International Conference on Mathematical Models and Methods in Applied Sciences, MMMAS*, 2014, p. 116.

[15] Korovkin N., Nitsch J., Solovyeva E., Examination of the Demodulation Effect of Two-Tone Disturbances on Nonlinear Elements, *Advances in Radio Science*, 2004, vol. 2, № 2, p. 51.

[16] Adalev A.S., Hayakawa M., Korovkin N.V., Identification of Electric Circuits Described by Ill-Conditioned Mathematical Models, *IEEE Transactions on Circuits and Systems I: Fundamental Theory and Applications*, Vol.53, № 1, 2006, pp. 78–91.

[17] Adalev A.S., Hayakawa M., Korovkin N.V., Identification of Electric Circuits: Problems and Methods of Solution Accuracy Enhancement, *Proceedings – IEEE International Symposium on Circuits and Systems, ISCAS*, 2005, pp. 980–983.

[18] Adalev A.S., Hayakawa M., Korovkin N.V., Using Linear Relations between Experimental Characteristics in Stiff Identification Problems of Linear Circuit Theory, *IEEE Transactions on Circuits and Systems I: Fundamental Theory and Applications*, Vol.55. № 5, 2008, pp. 1237–1247.

[19] Nikolay V. Silin, Nikolay V. Korovkin, Masashi Hayakawa, Electromagnetic Radiation from Power Equipments as Diagnostics of their Technical Evaluation, *J. Energy Power Sources*, Vol.1, No. 2, 2014, pp. 89–100.

[20] N.V. Silin, N.V. Korovkin, Electromagnetic monitoring of the power equipment, *Energetika*, No. 4, 2008, pp. 186–192.

[21] N.V. Silin, N.V. Korovkin, N.I. Ignatiev, I.V. Filimonov, High-voltage equipment electromagnetic control, *Int. Symp. On EMC EUROPE, Brugge, Belgium*, 2013, pp. 850–853.